References

AHMED, F. R. (1966). N.R.C. Crystallographic Programs for the IBM/360 system. Data Reduction and Structure Factor Least Squares.

AHMED, F. R. & BARNES, W. H. (1963). *Acta Cryst.* **16**, 1249.

AUER-WELSBACH, H., NOWOTNY, H. & KOHL, A. (1958). *Mh. Chem.*, **89**,154.

GAMBINO, R. J. (1967). *J. Less-Common Met.* **12**, 344.

HAMILTON, W. C. (1965). *Acta Cryst.* **18**, 502

IANDELLI, A. & BOTTI, F. (1937). *Atti reale Acad. nazl. Lincei*, **25**, 498.

International Tables for X-ray Crystallographic (1962). Vol. III. pp. 211, 213. Birmingham: Kynoch Press.

NORLING, B. K. & STEINFINK, H. (1966). *Inorg. Chem.* **5**, 1488.

PEARSON, W. B. (1965). *A Handbook of Lattice Spacing and Structures of Metals and Alloys*, Vol. 2. Toronto: Pergamon Press.

RIEGER, W. & PARTHÉ, E. (1968). *Acta Cryst.* B**24**, 456.

SATO, M., TAYLOR, J. B. & CALVERT, L. D. (1967). *J. Less-Common Met.* **12**, 419.

SMITH, D. K. (1967). Revised program for calculating X-ray powder diffraction patterns. UCRL-50264.

SMITH, D. K. (1968). *Norelco Reporter*, **15**, 57.

SWANSON, H. E., MORRIS, M. C., STINCHFIELD, R. P. & EVANS. E. H. (1962). *Nat. Bur. Stand. Monograph* 25 – Section 1,3.

VOGEL, R. & KLOSE, H. (1954). *Z. Metallk.* **45**, 633.

WANG, R. & STEINFINK, H. (1967). *Inorg. Chem.* **6**, 1685.

WANG, R., STEINFINK, H. & BRADLEY, W. F. (1966). *Inorg. Chem.* **5**, 142.

Acta Cryst. (1970). B26, 1540

The Crystal Structure of Anhydrous UO_2F_2*

BY M. ATOJI AND M. J. MCDERMOTT†

Chemistry Division, Argonne National Laboratory, Argonne, Illinois 60439, *U.S.A.*

(*Recieved* 25 *September* 1969)

A neutron powder-diffraction study of UO_2F_2 has been carried out. The structure is trigonal with a unit-layer unit cell with $a=b=4{\cdot}192\pm0{\cdot}001$ and $c/3=5{\cdot}220\pm0{\cdot}003$ Å and bonding distances of $U-O=1{\cdot}74\pm0{\cdot}02$ and $U-F=2{\cdot}429\pm0{\cdot}002$ Å, confirming essentially a previous X-ray study but with considerably higher accuracy. The powder sample consisted of approximately equal cumulative volumes of four different types of *ordered* coherent domains, containing individually the layer sequences, $A^+B^+C^+$, $A^-B^-C^-$, $A^+B^+A^+B^+C^+B^+C^+A^+C^+$ and $A^-B^-A^-B^-C^-B^-C^-A^-C^-$, where (+) and (−) refer respectively to the right-side-up and upside-down unit-layer configurations. In each layer sequence, a backward stacking with the opposite-sign unit layer is equally possible in powder diffractometry. All structures belong to the centric trigonal space group $R\bar{3}m$ (D^5_{3d}). The polymorphic, multidomain structure is not necessarily unique, although an exhaustive search for other probable models was fruitless.

Introduction

Zachariasen (1954) made a pioneering contribution to the structure chemistry of the $5f$ series of elements by solving the crystal structures of a number of actinide compounds using the X-ray diffraction method. His study included anhydrous uranyl fluoride, UO_2F_2, which was found to exhibit growth layer-stacking faults almost inherently (Zachariasen, 1948). Based on the X-ray powder data, Zachariasen assigned a rhombohedral structure with a cubic close-packing layer sequence to the *ideally* ordered UO_2F_2 and interpreted the stacking faults by introducing a hexagonal close-packing sequence with a random-walk probability. The stacking ordering increases with heat treatment, but the *ideally* ordered structure is hardly achievable in practice. Since neutron diffraction is more sensitive to the structure parameters of UO_2F_2, we have re-examined the subject using this technique. In this paper the rhombohedral crystal structure is conveniently described with reference to hexagonal axes unless otherwise stated.

Experimental

The anhydrous UO_2F_2 used in this work was prepared by treating UO_3 with gaseous anhydrous HF at temperatures between 350 and 500 °C in a nickel reactor (Hoekstra, 1963). Chemical analysis of the samples confirmed the stoichiometry, as indicated by a satisfactory agreement between the observed and calculated weight percentages (the latter values in parentheses), uranium $77{\cdot}1\pm0{\cdot}1$ (77·28), oxygen $10{\cdot}3\pm0{\cdot}1$ (10·39)

---

* Work performed under the auspices of the U.S. Atomic Energy Commission.

† Present address: Imperial Chemical Industries Limited, Petrochemical and Polymer Laboratory, P.O. Box 11, The Heath, Runcorn, Cheshire, England.

and fluorine 12·5 ± 0·1 (12·34). Spectroscopic analysis did not detect any metallic impurity in excess of 200 p.p.m. Thermal decomposition of UO_2F_2 above about 700°C (Ferris & Baird, 1960) precludes the use of various known high-temperature crystal-growth techniques and the absence of appropriate non-aqueous solvents for anhydrous UO_2F_2 inhibits the single-crystal preparation from solutions. Consequently, only powder specimens have been used in this work. Anhydrous UO_2F_2 is hygroscopic and hence was handled in a dry, inert atmosphere. The average size of the UO_2F_2 crystallites in our powder samples was about several microns in diameter.

The neutron diffraction data were taken at room temperature, using a multipurpose automatic neutron diffractometer (Atoji, 1965) with a wavelength setting of 1·069 Å. The sample was encased in a cylindric sample holder (1 cm in diameter) fabricated from a Ti–Zr alloy having zero coherent scattering amplitude. A diffraction pattern was also obtained for a mixture of UO_2F_2 and annealed aluminum filings. This mixture was used in order to verify the absence of detectable preferred orientation in the sample containing only UO_2F_2, and also to provide fiducial references for the UO_2F_2 lattice constant determination.

Basic structure

Our neutron diffraction pattern (Fig. 1) appears to be analogous to the X-ray pattern of a well heat-treated sample presented by Zachariasen (1948). Accordingly, the coherent peaks were initially indexed on the basis of the ordered rhombohedral structure proposed in that paper. Hence, the observable reflections should satisfy $-H+K+L=3n$ (H,K,L and n being integers) in the hexagonal indices. A Gaussian peak analysis reported previously (Atoji & Williams, 1961) was extensively employed for resolving the overlapped reflections. As in the case of the X-ray work (Zachariasen, 1948) it was found that the peak profiles of the reflections for $H-K=3n$ and $L=3n'$ were of 'sharp' Gaussian form, in accordance with the angular-resolution function of the diffractometer, whereas all other peaks exhibited considerable broadening and some of these 'diffuse' peaks appear to be shifted from their anticipated angles. For this reason, the 'sharp' peaks were used in the lattice constant determination. The measured lattice parameters, based on an analysis of six peaks in each of three separate diffraction patterns, were $a(=b)=4{\cdot}192 \pm 0{\cdot}001$ and $c=15{\cdot}66 \pm 0{\cdot}01$ Å, the quoted uncertainties here, as throughout this work, being standard deviations. The hexagonal-based unit-cell contains three UO_2F_2 formula units and the calculated density is 6·438 g.cm^{-3}. The equivalent rhombohedral unit-cell possesses $a_r=5{\cdot}754 \pm 0{\cdot}003$ Å and $\alpha=42°44' \pm 2'$, and contains one UO_2F_2 unit. Zachariasen (1948) has reported $a=4{\cdot}206 \pm 0{\cdot}001$ and $c=15{\cdot}69 \pm 0{\cdot}01$ Å, both of which are slightly different from our values. It is likely that the lattice parameters of UO_2F_2 are sample-dependent. The coherent neutron scattering amplitudes adopted for the intensity calculations were 0·845 for U (Atoji, 1966), 0·58 for O and 0·56 for F, all in 10^{-12} cm (Bacon, 1962).

The structure description of UO_2F_2 is greatly facilitated by use of the layer unit-cell constituted by a, b and $c/3$. The least-squares and R-index curve (Atoji, Gschneidner, Duane, Rundle & Spedding 1958) analyses on the integrated intensities of the sharp reflections led to the layer unit-cell coordinates on the basis of a, b and c, (000) for uranium, $\pm(00z_0)$ with $z_0=0{\cdot}1110\ (\simeq\frac{1}{9}) \pm 0{\cdot}0015$ for oxygen and $\pm(\frac{2}{3},\frac{1}{3},z_F)$ with $z_F=\pm(0{\cdot}0133 \pm 0{\cdot}0015)$ for fluorine. In accordance with the sign of z_F given above, the atomic arrangements with two alternative fluorine coordinates are hereafter distinguished by the (+) and (−) notations on the structure terminologies. The temperature factor coefficient was found to be $2B=3{\cdot}1 \pm 0{\cdot}3$ Å^2; this value has also been applied to the calculated 'diffuse' peak intensities. Zachariasen (1948) reported values of $z_0=0{\cdot}122$ and $z_F=0{\cdot}039$, both of which are significantly different from our values. Actually, the 'sharp' reflection data are invariant with any choice among $\pm z$, $\frac{1}{3}\pm z$ and $\frac{2}{3}\pm z$ for a given z value. The foregoing coordinates were chosen by assuming the existence of the strongly bonded uranyl groups in UO_2F_2 and also from the steric-hindrance consideration in the layer stacking. These choices were later substantiated by the intensity analysis on the 'diffuse' reflections.

The U−O bonding distance in UO_2F_2 is 1·74 ± 0·02 Å, which compares favorably with U−O = 1·71 Å obtained from infrared frequency analysis of UO_2F_2 (Hoekstra, 1963) and also with U−O = 1·71 ± 0·04, 1·78 ± 0·02 and 1·76 ± 0·01 Å determined by means of single-crystal neutron diffraction studies of uranyl acetate (Zachariasen & Plettinger, 1959), $RbUO_2(NO_3)_3$ (Barclay, Sabine & Taylor 1965), and $[UO_2(NO_3)_2(H_2O)_2]4H_2O$ (Taylor & Mueller, 1965), respectively. The trigonal layer of UO_2F_2 is a slightly puckered plane with the oxygen atoms in a dumb-bell configuration perpendicular to this plane, and the fluorine atoms situated 0·21 ± 0·02 Å alternately above and below the median layer plane formed by the uranium atoms. Each layer is tightly packed through the interatomic distances U−6F = 2·429 ± 0·002, F...3F′ = 2·456 ± 0·006, O...F = 2·86 ± 0·02 and O...3F′ = 3·11 ± 0·02 Å. The (−) layer is an upside-down configuration of the (+) layer.

Layer stacking

The intensity of a sharp reflection is also invariant with the layer unit-cell translations of $\mp\frac{\mathbf{a}}{3} \pm \frac{\mathbf{b}}{3}$ ($|\mathbf{a}|=a$ and $|\mathbf{b}|=b$), so long as the neighboring layer spacing is equal to $c/3$. We denote the origin layer as A, the layer generated by A plus $\left(-\frac{\mathbf{a}}{3}+\frac{\mathbf{b}}{3}\right)$ as B and that by A plus $\left(+\frac{\mathbf{a}}{3}-\frac{\mathbf{b}}{3}\right)$ as C. The sharp-reflection-only analysis cannot distinguish the layer stackings consisting of any choices or combinations among A^+, B^+, C^+, A^-, B^- and C^-. However, the A^+A^+ or A^+A^- type sequence is highly unlikely, since the interlayer oxygen–oxygen distance becomes an unrealistically short 1·74 Å. Also, the relatively strong observed intensities of the 'diffuse' peaks readily discount such uncommon layer sequences.

The foregoing ambiguities should be at least partly resolved by the 'diffuse' peak analysis. An important ambiguity nevertheless should always remain because of the multiplet characteristics of the individual powder reflection. A simple example is that powder diffractometry cannot distinguish between the $(A^+B^+C^+)$ and $(A^-C^-B^-)$ stackings, where the repetition-unit sequence is bracketed. In general, a given (+) layer stacking and its backward-sequence of the (−) layers give rise to the same powder intensity at the same scattering angle, regardless of the degree of disordering.

The interlayer separation is due chiefly to the oxygen–oxygen approach distance of $O\cdots 3O' = 2{\cdot}98 \pm 0{\cdot}02$ Å which approximates closely the van der Waals or ionic contact distance of 2·8 Å. The interlayer $O\cdots F$ distance in the direction of the c axis is $3{\cdot}27 \pm 0{\cdot}03$ or $3{\cdot}68 \pm 0{\cdot}03$ Å and the next closest $O\cdots 3F'$ distance is 4·41 or 4·07 Å, for the A^+B^+ or A^-B^- type sequences respectively. In both the (+) and (−) structures, the closest interlayer $F\cdots F'$ distance is 5·38 Å, while the van der Waals or ionic radius of F is around 1·35 Å. Consequently, the interatomic distance consideration is unable to provide any substantive criterion in discriminating between the (+) and (−) structures.

We have examined systematically practically all conceivable stacking sequences, consisting of all or part of weighted combinations of the six different unit-layers, with or without stacking faults, utilizing the diffraction formalisms developed by a number of authors for the one-dimensional disordering and antiphase-domain structures (Holloway & Klamkin, 1969 and the references therein; Gevers, 1954; Fujiwara, 1957). Analyses of this sort often lead to ambiguous results. However, all but one model could readily be discarded through the curve fitting to a few observed 'diffuse' peaks at low angles (particularly

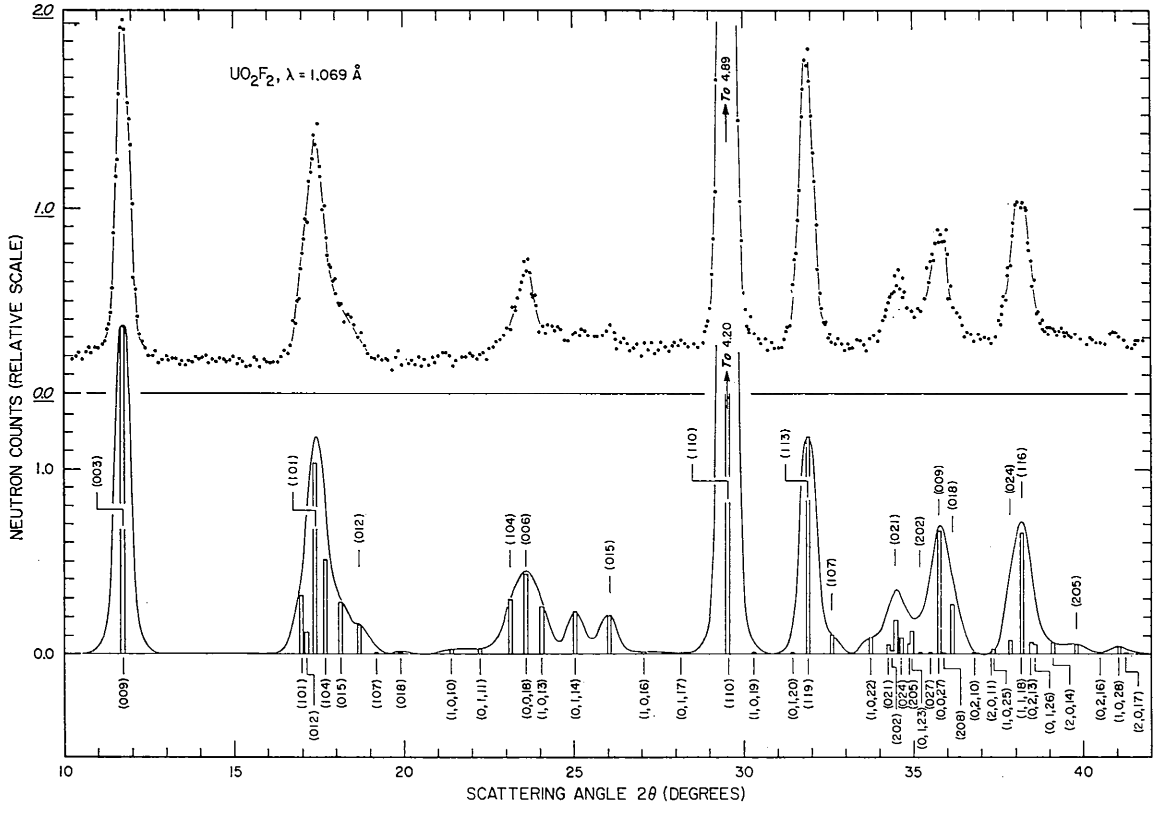

Fig. 1. One of the observed diffraction patterns of UO_2F_2 shown in the upper-half section is compared with the calculated diffraction pattern based on the proposed multidomain structure. In the latter pattern, the indices placed above and in the background refer to the (ABC) and ($ABABCBCAC$) structures respectively. The calculated heights of the Gaussian peaks are shown by bars and the envelope of the calculated Gaussian peaks is shown by the solid line. No coherent peaks were detectable below 10° in 2θ.

those given in Fig. 2), although our best model described below is not necessarily unique. The model used by Zachariasen (1948), involving the formalism presented in detail in a later paper (Zachariasen, 1967), is incompatible with the data which were obtained with our sample.

Our UO_2F_2 sample consists of the following four different ordered-sequence-group structures;

$$\begin{cases}(1a) & (A^+B^+C^+)\,,\\(1b) & (A^-C^-B^-)\,,\end{cases}$$
$$\begin{cases}(2a) & (A^-B^-C^-)\,,\\(2b) & (A^+C^+B^+)\,,\end{cases}$$
$$\begin{cases}(3a) & (A^+B^+A^+B^+C^+B^+C^+A^+C^+)\,,\\(3b) & (A^-C^-A^-C^-B^-C^-B^-A^-B^-)\,,\end{cases}$$
$$\begin{cases}(4a) & (A^-B^-A^-B^-C^-B^-C^-A^-C^-)\,,\\(4b) & (A^+C^+A^+C^+B^+C^+B^+A^+B^+)\,.\end{cases}$$

This particular structure model was deduced as follows: It was found that many features of the observed diffraction pattern could be explained by an antiphase domain structure with a modulation period of $3|c|$ indicating a nine-layer repetition sequence. Moreover, it was necessary to retain a similar cumulative volume for the three-layer sequence structure in order to account qualitatively for the diffraction intensities. This implied that the sample consisted of structures (1*a*) and (3*a*). A superior fit was achieved when the (−)-layer variants of the above, (2*a*) and (4*a*) respectively, were included. As mentioned earlier, the (−)-layer backward stacked version of a particular (+)-layer sequence is indistinguishable from the given (+)-layer, thus the '*b*' variants cannot be excluded. It should be emphasized that, in contrast with the Zachariasen model (1948), all eight probable structures, (1*a*) through (4*b*), give rise to the 'sharp' reflections. There exists little or no coherence between any two of the eight different structures in the scattering process. We denote the cumulative volume of the coherent domains occupied by the structure (1*a*) as $V(1a)$, for instance. We found that in our powder samples $V(1a)+V(1b)\simeq V(2a)+V(2b)\simeq V(3a)+V(3b)\simeq V(4a)+V(4b)$. All of the individual layer sequences, (1*a*) through (4*b*), belong to the centric space group, D^5_{3d} – $R\bar{3}m$. The rhombohedral unit-cell dimensions for (3*a*) through (4*b*) are $a_r=15{\cdot}84\pm0{\cdot}01$ Å and $\alpha=21°22'\pm6'$.

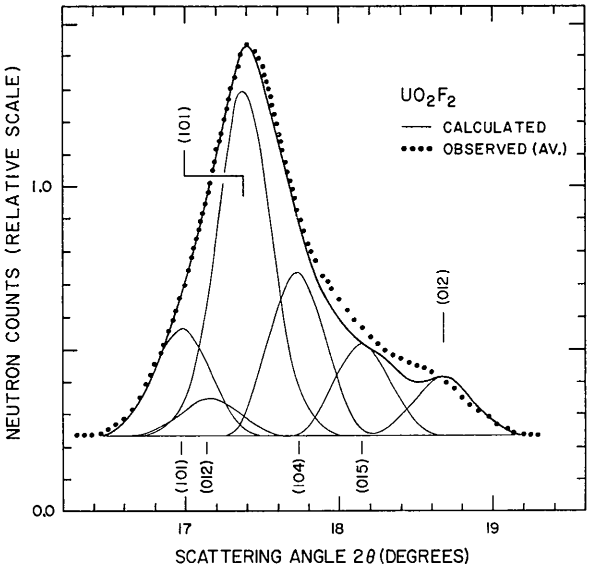

Fig. 2. The most reliable, observed 'diffuse' peak data (an average of three scannings) are compared with the calculated Gaussian line profiles whose individual and composite values are outlined by fine and heavy solid lines respectively. The indexing convention is the same as that in Fig. 1.

For the cumulative structure consisting of (1*a*), (2*a*), (3*a*) and (4*a*), the coherently diffracted intensity per UO_2F_2 is given by

$$I_{\text{calc}}=\frac{j\text{L}}{4}\,[Q_1^2\{(F^+)^2+(F^-)^2\}+Q_2^2\{(F^+)^2+(F^-)^2\}]\times\exp\,[-2B(\sin\theta/\lambda)]^2\,.$$

Here, j is the multiplicity factor; L is the Lorentz factor; the four addition terms represent (1*a*), (2*a*), (3*a*) and (4*a*) in that order; F^+ and F^- are the layer structure factors per UO_2F_2 for the (+) and (−) layers, respectively:

$$Q_1^2=\tfrac{1}{9}\left\{1+2\cos 2\pi\left(\frac{H-K-L}{3}\right)\right\}^2$$

and

$$Q_2^2=\frac{1}{81}\left\{1+2\cos 2\pi\left(\frac{H-K}{3}-\frac{L'}{9}\right)+2\cos 2\pi\frac{2L'}{9}+2\cos 2\pi\left(\frac{H-K-L'}{3}\right)+2\cos 2\pi\left(\frac{H-K}{3}+\frac{4L'}{9}\right)\right\}^2.$$

The numerical values of Q_1^2 and Q_2^2 are as follows:

$$Q_1^2=\begin{cases}1, \text{ for } -H+K+L=3n,\\0, \text{ otherwise.}\end{cases}$$

$$Q_2^2\begin{cases}1, \text{ for } H-K=3n \text{ and } L'=9n'\\0, \text{ for } H-K=3n \text{ and } L'\neq 9n'; \text{ and for}\\-H+K+L'\neq 3n\,.\\0{\cdot}0859, \text{ for } \begin{cases}H-K=3n+1 \text{ and } L'=9n'+2\,,\\H-K=3n-1 \text{ and } L'=9n'+7\,.\end{cases}\\0{\cdot}7123, \text{ for } \begin{cases}H-K=3n+1 \text{ and } L'=9n'+5\,,\\H-K=3n-1 \text{ and } L'=9n'+4\,.\end{cases}\\0{\cdot}2017, \text{ for } \begin{cases}H-K=3n+1 \text{ and } L'=9n'+8\,,\\H-K=3n-1 \text{ and } L'=9n'+1\,,\end{cases}\end{cases}$$

where L and L' refer to c and $3c$, respectively. For the cumulative structure composed of (1*b*), (2*b*), (3*b*) and (4*b*), both H and K as well as the superscripts of both F^+ and F^- should take the opposite signs.

Satisfactory agreements between the observed and calculated values are seen in Figs. 1 and 2, where the scaling for the calculated values is given by $[0{\cdot}25\times10^{-2}\,I_{\text{calc}}]/W$. The W is the full-width in $2\theta°$ at half height of the Gaussian powder line profile. The scattering-angle dependency of the empirical W as determined from the diffraction patterns of various powder specimens is approximated by (with maximum error of ±5% in average) $W=(0{\cdot}306t^2-0{\cdot}427t+0{\cdot}333)^{1/2}$, where $t=\tan\theta/\tan\theta_m$ with $\theta_m=14{\cdot}83°$ representing the Bragg angle of the copper neutron monochromator (Caglioti, Paoletti & Ricci, 1958).

The 9-layer repetition sequence, [*ABABCBCAC*], has also been found in samarium metal (Ellinger & Zachariasen, 1953; Daane, Rundle, Smith & Spedding 1954) and in a ternary Laves phase having approximate composition MgCuAl (Komura, 1962). Stacking faults or disorderings in less-heat-treated UO_2F_2 may be most properly interpreted using the method similar to that used in the MgCuAl case.

References

Atoji, M. (1965). *Nucl. Instr. Methods,* **35**, 13; Argonne National Laboratory Rept. No. 6920 (1964).

Atoji, M. (1966). *Acta Cryst.* **20**, 587.

Atoji, M. & Williams, D. E. (1961). *J. Chem. Phys.* **35**, 1960.

Atoji, M., Gschneidner, K. Jr, Daane, A. H., Rundle, R. E. & Spedding, F. H. (1958). *J. Amer. Chem. Soc.* **80**, 1804.

Bacon, G. E. (1962). *Neutron Diffraction,* 2nd ed. p. 275. Oxford: Clarendon Press.

Barclay, G. A., Sabine, T. M. & Taylor, J. C. (1965). *Acta Cryst.* **19**, 205.

Caglioti, G., Paoletti, A. & Ricci, F. P. (1958). *Nucl. Inst. Methods,* **3**, 223.

Daane, A. H., Rundle, R. E., Smith, H. G. & Spedding, F. H. (1954). *Acta Cryst.* **7**, 532.

Ellinger, F. H. & Zachariasen, W. H. (1953). *J. Amer. Chem. Soc.* **75**, 5650.

Ferris, L. M. & Baird, F. G. (1960). *J. Electrochem. Soc.* **107**, 305.

Fujiwara, K. (1957). *J. Phys. Soc. Japan,* **12**, 7.

Gevers, R. (1954). *Acta Cryst.* **7**, 337.

Hoekstra, H. R. (1963). *Inorg. Chem.* **2**, 492.

Holloway, H. & Klamkin, M. S. (1969). *J. Appl. Phys.* **40**, 1681.

Komura, Y. (1962). *Acta Cryst.* **15**, 770.

Taylor, J. C. & Mueller, M. H. (1965). *Acta Cryst.* **19**, 536.

Zachariasen, W. H. (1948). *Acta Cryst.* **1**, 277.

Zachariasen, W. H. (1954). *Acta Cryst.* **7**, 795.

Zachariasen, W. H. (1967). *Acta Cryst.* **23**, 44.

Zachariasen, W. H. & Plettinger, H. A. (1959). *Acta Cryst.* **12**, 526.

Acta Cryst. (1970). **B26**, 1544

Zur Kristallstruktur des $ZnCl_2.\frac{1}{2}HCl.H_2O$

Von Heinz Follner

Mineralogisch-Kristallographisches Institut der Technischen Universität,
3392 *Clausthal-Zellerfeld, Sägemüllerstrasse* 4, *Deutschland*

(*Eingegangen am* 11. *Juli* 1969)

$ZnCl_2.\frac{1}{2}HCl.H_2O$ crystallizes from aqueous solutions containing hydrochloric acid with unit-cell dimensions $a_0=9{\cdot}26$, $b_0=22{\cdot}90$, $c_0=8{\cdot}91$ Å, space group *Fdd*2 with $Z=16$. The structure was solved by direct methods and by Patterson syntheses. By least-squares methods with individual isotropic temperature factors and individual weights the structure was refined to $R_1=9{\cdot}7\%$. Zinc is tetrahedrally coordinated by four chlorine atoms.

Einleitung

Salzsaure Zinkchloridhydrate der Zusammensetzungen $ZnCl_2.\frac{1}{2}HCl.H_2O$ und $ZnCl_2.HCl.2H_2O$ sind seit längerem bekannt (Engel, 1886, 1889; Tschelzow, 1887; Weitz & Stamm, 1929). Im Rahmen der Bearbeitung von Kristallstrukturen der Zinkhalogenidhydrate wurde die Strukturaufklärung des $ZnCl_2.\frac{1}{2}HCl.H_2O$ durchgeführt.

Experimentelles

$ZnCl_2.\frac{1}{2}HCl.H_2O$ wurde bei Zimmertemperatur aus einer salzsauren Zinkchloridlösung in Form von rhomboederähnlichen Kristallen erhalten. Aus Precessionaufnahmen ergaben sich folgende Gitterkonstanten:

$$a=9,26\pm0,05\ \text{Å}$$
$$b=22,90\pm0,12$$
$$c=8,91\pm0,05\,.$$

Der Zellinhalt beträgt 16 Formeleinheiten. Die Auslöschungen der Reflexe sind charakteristisch für die Raumgruppe *Fdd*2. Die Röntgeninterferenzen wurden nach dem Weissenberg-equi-inclination-Verfahren mit automatischer Messroutine und monochromatisierter